

The effect of assimilation, fractional crystallization, and ageing on U-series disequilibria in subduction zone lavas

Fang Huang*, Lili Gao, Craig C. Lundstrom

Department of Geology, University of Illinois at Urbana-Champaign, 1301 W. Green Street, IL 61801, USA

Received 22 October 2007; accepted in revised form 27 May 2008; available online 14 June 2008

Abstract

Although most arc lavas have experienced significant magma differentiation, the effect of the differentiation process on U-series disequilibria is still poorly understood. Here we present a numerical model for simulating the effect of time-dependent magma differentiation processes on U-series disequilibria in lavas from convergent margins. Our model shows that, in a closed system with fractional crystallization, the ageing effect can decrease U-series disequilibria via radioactive decay while in an open system, both ageing and bulk assimilation of old crustal material serve to reduce the primary U-series disequilibria. In contrast, with recharge of refresh magma, significant ^{226}Ra excess in erupted lavas can be maintained even if the average residence time is longer than 8000 years.

The positive correlations of ($^{226}\text{Ra}/^{230}\text{Th}$) between Sr/Th or Ba/Th in young lavas from convergent margins have been widely used as evidence of fluid addition generating the observed ^{226}Ra excess in subduction zones. We assess to what extent the positive correlations of ($^{226}\text{Ra}/^{230}\text{Th}$) with Sr/Th and Ba/Th observed in the Tonga arc could reflect AFC process. Results of our model show that these positive correlations can be produced during time-dependent magma differentiation at shallow crustal levels. Specifically, fractional crystallization of plagioclase and amphibole coupled with contemporaneous decay of ^{226}Ra can produce positive correlations between ($^{226}\text{Ra}/^{230}\text{Th}$) and Sr/Th or Ba/Th (to a lesser extent). Therefore, the correlations of ($^{226}\text{Ra}/^{230}\text{Th}$) with Sr/Th and Ba/Th cannot be used to unambiguously support the fluid addition model, and the strength of previous conclusions regarding recent fluid addition and ultra-fast ascent rates of arc magmas is significantly lessened.

© 2008 Published by Elsevier Ltd.

1. INTRODUCTION

Convergent margins play a critical role in Earth's geochemical cycling, crust-mantle interactions and generation of new continental crust. During subduction, hydrous fluids are released from the subducted oceanic slab and added to the overlying mantle wedge. In response to the addition of water, partial melting of mantle peridotite produces H_2O rich subduction zone magmas (e.g., Gill, 1981; Grove and Kinzler, 1986; Grove et al., 2006). Because parent-daughter disequilibrium will decay back to secular equilibrium in ~ 5 half-lives of a daughter nuclide, U-series disequilibria are

powerful tools for constraining the time-scale of subduction zone magmatism. Hundreds of U-series analyses for convergent margin lavas have now been reported (see Turner et al. (2003) for a recent review) leading to four important general observations: (1) most young lavas have ^{238}U excess over ^{230}Th but a substantial number also have ^{238}U depletion or ^{238}U – ^{230}Th equilibrium (e.g., Turner et al., 1996, 2003; Sigmarsson et al., 2002; Dosseto et al., 2003); (2) almost all young lavas have ^{231}Pa excess over ^{235}U (Pickett and Murrell, 1997; Bourdon et al., 1999; Thomas et al., 2002; Dosseto et al., 2003; Turner et al., 2006; Huang and Lundstrom, 2007); (3) most lavas have ^{226}Ra excesses which negatively correlate with SiO_2 content and positively correlated with Sr/Th or Ba/Th (Turner et al., 2000, 2001; Turner and Foden, 2001); and (4) convergent margin lavas on average have higher U/Th than MORB (Turner et al., 2003).

* Corresponding author.

E-mail addresses: fhuang1@uiuc.edu, huangfang426@hotmail.com (F. Huang).

Most lavas at convergent margins do not represent primitive magmas but instead have experienced significant crustal level differentiation (e.g., Gill, 1981). A number of studies have emphasized the importance of fractional crystallization and assimilation of crustal materials in generating the compositional variations in subduction zone magmas (e.g., DePaolo, 1981; Hildreth and Moorbath, 1988; Beard et al., 2005). DePaolo (1981) provided equations for quantifying the geochemical effects of assimilation and fractional crystallization (AFC) and applied them to open-system magma evolution. Because U-series nuclides usually have small partition coefficients (<0.01) between most silicate minerals and melt (Blundy and Wood, 2003), fractional crystallization by itself should not significantly affect U-series disequilibria generated by earlier magmatic processes (such as melting or fluid addition). However, because magma residence times could vary from tens of years to 10^5 years (e.g., Halliday et al., 1989; Heath et al., 1998; Hawkesworth et al., 2000; Zellmer et al., 2000; Cooper et al., 2001; Condomines et al., 2003; Reagan et al., 2003; Asmerom et al., 2005; Jicha et al., 2005), contemporaneous decay of short-lived nuclides (such as ^{226}Ra) during AFC processes could significantly affect the extent of U-series disequilibria in young lavas (Condomines et al., 1995). Indeed, previous works have addressed the variation of ($^{226}\text{Ra}/^{230}\text{Th}$) due to fractional crystallization and magma replenishment for the case of the Ardoukoba Volcano (Asal rift, Djibouti) (Vigier et al., 1999) and variation of ($^{226}\text{Ra}/^{230}\text{Th}$) with time in a closed system to constrain the cooling rate of magma chambers (Blake and Rogers, 2005). Besides the effect of fractional crystallization, ageing, and replenishment (Hughes and Hawkesworth, 1999; Hawkesworth et al., 2000), U-series disequilibria can also be changed by addition of assimilation of crustal materials. Recently, Touboul et al. (2007) reported a model simulating U-series disequilibrium variations in closed and open systems assuming that crystallization rate is a linear function of the mass of magma in the chamber which exponentially decreases with time.

In this paper, we present a more general time-dependent AFC model assuming a constant rate of change for magma mass with time. This model can be used to simulate the variation in U-series disequilibria due to assimilation of crustal materials, fractional crystallization, and magma recharge coupled with ageing. It allows for simulation of both closed and open system (assimilation and recharge) behavior and accounts for decay of short-lived U-series nuclides in the calculation. The aim of this model is to provide a tool for better assessing the effect of magma differentiation processes on U-series disequilibria and to provide an alternative explanation for the positive correlations between ^{226}Ra excess and Sr/Th or Ba/Th.

2. EQUATIONS FOR TIME-DEPENDENT AFC MODEL

Our model follows the basic equations of DePaolo (1981), starting with a general scenario including assimilation, fractional crystallization, and continuous recharge (AFCR) processes. As magma accumulates in a crustal level

magma chamber (Fig. 1), its mass changes according to the equation: $dM_m/dt = M'_a + M'_r - M'_c$, where M_m is the total mass of magma in the chamber, M'_c is the mass change rate by fractional crystallization, M'_a is the rate of change of mass due to assimilation, and M'_r is the rate of change of mass due to recharge. If there is no recharge of fresh magma, the AFCR model reduces to AFC, which reduces further to pure fractional crystallization (FC) model if the rate of assimilation is zero. A description of nomenclatures and parameters used is given in Table 1.

2.1. Trace element concentrations

Similar to equation 1a of DePaolo (1981), we assume that the concentration of a trace element in the recharging magma is constant (C_m^0) such that the instantaneous rate of change of mass of a trace element is given by:

$$\begin{aligned} \frac{d(M_m C_m)}{dt} &= C_m \frac{dM_m}{dt} + M_m \frac{dC_m}{dt} \\ &= M'_a C_a + M'_r C_m^0 - M'_c D C_m \end{aligned} \quad (1)$$

where C_m is the concentration of the trace element and D is the bulk partition coefficient of the element between the crystallized minerals and melt.

If $\frac{dM_m}{dt} = 0$, magma evolution is similar to a zone refining process, where the mass of the magma chamber is always M_m^0 . Eq. (1) can be integrated as:

$$C_m = \left(C_m^0 - \frac{r_a C_a + r_r C_m^0}{r_c D} \right) e^{-r_c D t} + \frac{r_a C_a + r_r C_m^0}{r_c D} \quad (2)$$

where $r_a = \frac{M'_a}{M_m^0}$, defined as the assimilation rate, $r_r = \frac{M'_r}{M_m^0}$, the recharge rate, and $r_c = \frac{M'_c}{M_m^0}$, the crystallization rate.

In general, $\frac{dM_m}{dt} \neq 0$. For a slowly cooling magma chamber, $\frac{dM_m}{dt} < 0$. Eq. (1) can be re-written as:

$$\frac{dC_m}{d \ln F} + \left(1 + \frac{r_c D}{r_a + r_r - r_c} \right) C_m = \frac{r_a C_a + r_r C_m^0}{r_a + r_r - r_c} \quad (3)$$

where F is the fraction of melt remaining in the magma chamber ($F = \frac{M_m}{M_m^0}$); and $dF = \frac{M'_a + M'_r - M'_c}{M_m^0} dt = (r_a + r_r - r_c) dt$. An analytical solution for Eq. (3) is:

$$C_m = C_m^0 F^{-\frac{r_a + r_r - r_c + r_c D}{r_a + r_r - r_c}} + \frac{r_a C_a + r_r C_m^0}{r_a + r_r - r_c + r_c D} \left(1 - F^{-\frac{r_a + r_r - r_c + r_c D}{r_a + r_r - r_c}} \right) \quad (4)$$

If $r_r = 0$, Eq. (5) is same to equation (6a) in DePaolo (1981).

2.2. Short-lived U-series nuclides

If the residence time of magma is comparable to or longer than the half-lives of the short-lived isotopes, radioactive decay must be taken into account for assessing the change of mass in U-series nuclides in a magma chamber. The variation of mass of a daughter nuclide with time can be written as:

$$\begin{aligned} \frac{d(M_m C_{m,D})}{dt} &= M'_a C_{a,D} + M'_r C_{m,D}^0 - M'_c D_D C_{m,D} \\ &\quad + \frac{\lambda_P M_m m_D C_{m,P}}{m_P} - \lambda_D M_m C_{m,D} \end{aligned} \quad (5)$$

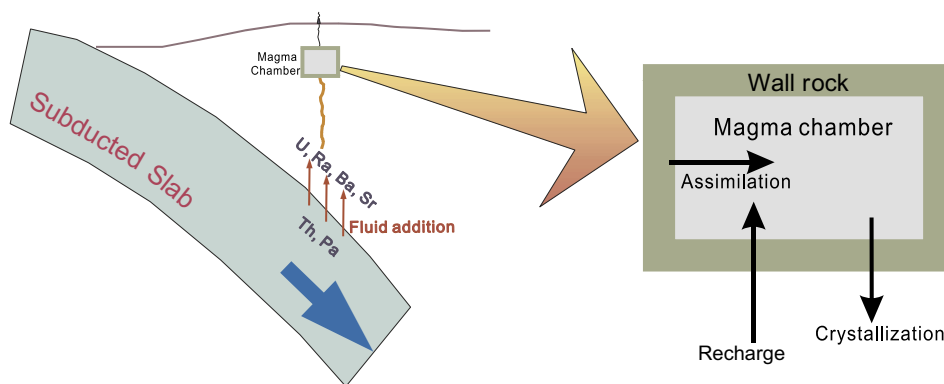


Fig. 1. Cartoon for subduction zone and magma chamber at crustal depths. Mantle wedge is metasomatised by hydrous fluid enriched in U, Ra, Ba, and Sr relative to Th and Pa. Mass and chemical composition of magma chamber vary due to assimilation, crystallization, and recharge.

Table 1
Parameters for the models

Symbol	Description	Units
M_m	Mass of magma	kg
M_m^0	Initial mass of magma	kg
m_P	Atomic mass for parent	—
m_D	Atomic mass for daughter	—
M'_a	Mass change rate due to assimilation	kg/ year
M'_r	Mass change rate due to continuous recharge	kg/ year
M'_c	Mass change rate due to fractional crystallization	kg/ year
r_a	M'_a/M_m^0 , assimilation rate	year ⁻¹
r_r	M'_r/M_m^0 , continuous recharge rate	year ⁻¹
r_c	M'_c/M_m^0 , fractional crystallization rate	year ⁻¹
F	Fraction of magma, M_m/M_m^0	—
C_m	Concentration in magma	ppm
$C_{m,D}$	Concentration of daughter nuclides in magma	ppm
$C_{m,P}$	Concentration of parent nuclides in magma	ppm
C_a	Concentration in assimilated materials	ppm
$C_{a,D}$	Concentration of daughter nuclides in assimilated materials	ppm
Γ	$\Gamma = \frac{1}{r_a+r_r-r_c}$, $-\Gamma$ is residence time	years
D	Bulk partition coefficient between magma and fractionated phases	—
D_D	Partition coefficient of daughter	—
D_P	Partition coefficient of parent	—

where $C_{a,D}$ is the concentration of the daughter in the assimilated materials; λ_D and λ_P are the decay constants of the daughter and parent, respectively; D_D is the bulk partition coefficient of daughter; $C_{m,D}^0$ is the initial concentration of daughter in the melt; $C_{m,P}$ is the concentration of parent in the melt; and m_D and m_P are the atomic mass of the daughter and parent, respectively.

If $\frac{dM_m}{dt} = 0$ or $r_a + r_r = r_c$, Eq. (5) reduces to

$$\begin{aligned} \frac{dC_{m,D}}{dt} &= \frac{M'_a C_{a,D} + M'_r C_{m,D}^0 - M'_c D_D C_{m,D}}{M_m^0} + \frac{\lambda_P m_D C_{m,P}}{m_P} - \lambda_D C_{m,D} \\ &\Rightarrow \frac{dC_{m,D}}{dt} + (\lambda_D + r_c D_D) C_{m,D} \\ &= r_a C_{a,D} + r_r C_{m,D}^0 + \frac{\lambda_P m_D C_{m,P}}{m_P} \end{aligned} \quad (6)$$

$C_{m,P}$ can be obtained from Eq. (2) if the daughter is ^{230}Th or ^{231}Pa .

$$\begin{aligned} \frac{dC_{m,D}}{dt} + (\lambda_D + r_c D_D) C_{m,D} \\ &= \frac{\lambda_P m_D}{m_P e^{r_c D_P t}} \left(C_{m,P}^0 - \frac{r_a C_{a,P} + r_r C_{m,P}^0}{r_c D_P} \right) + r_a C_{a,D} + r_r C_{m,D}^0 \\ &\quad + \lambda_P \frac{(r_a C_{a,P} + r_r C_{m,P}^0) m_D}{r_c D_P m_P} \end{aligned} \quad (7)$$

An analytical solution for Eq. (7) is:

$$\begin{aligned} C_{m,D} &= \frac{r_a C_{a,D} + r_r C_{m,D}^0 + \frac{\lambda_P m_D (r_a C_{a,P} + r_r C_{m,P}^0)}{m_P r_c D_P}}{\lambda_D + r_c D_D} (1 - e^{-(\lambda_D + r_c D_D)t}) \\ &\quad + \frac{\frac{\lambda_P m_D}{m_P} \left(C_{m,P}^0 - \frac{r_a C_{a,P} + r_r C_{m,P}^0}{r_c D_P} \right) (e^{-(\lambda_D + r_c D_D)t} - e^{-r_c D_P t})}{r_c D_P} \\ &\quad + C_{m,D}^0 e^{-(\lambda_D + r_c D_D)t} \end{aligned} \quad (8)$$

$C_{m,^{230}\text{Th}}$ and $C_{m,^{231}\text{Pa}}$ can be calculated using Eq. (8) assuming the parent nuclides are ^{238}U and ^{235}U , respectively, and ^{226}Ra , the daughter of ^{230}Th , can be obtained by substituting $C_{m,^{230}\text{Th}}$ as $C_{m,P}$ into Eq. (6).

The calculation is more complicated for the general case where $\frac{dM_m}{dt} \neq 0$. Eq. (5) can be written as:

$$\begin{aligned} \frac{dC_{m,D}}{dt} + \left(\frac{M'_a + M'_r - M'_c}{M_m} + \lambda_D + \frac{M'_c D_D}{M_m} \right) C_{m,D} \\ &= \frac{M'_a C_{a,D} + M'_r C_{m,D}^0}{M_m} + \frac{\lambda_P m_D C_{m,P}}{m_P} \end{aligned} \quad (9)$$

which is further reduced to:

$$\begin{aligned} \frac{dC_{m,D}}{dF} + \left(\frac{1}{F} + \lambda_D \Gamma + \frac{r_c D_D}{F(r_a + r_r - r_c)} \right) C_{m,D} \\ &= \frac{r_a C_{a,D} + r_r C_{m,D}^0}{F(r_a + r_r - r_c)} + \frac{\lambda_P m_D \Gamma C_{m,P}}{m_P} \end{aligned} \quad (10)$$

where $\Gamma = \frac{M_m^0}{M'_a + M'_r - M'_c} = \frac{1}{r_a + r_r - r_c}$ and $dt = \Gamma dF$. Note that Γ is the residence time of melt in the magma chamber. There is no analytical solution for Eq. (10). We used numerical

methods in MatLab to calculate the concentration of ^{230}Th or ^{231}Pa in the melt after obtaining the parent concentrations (^{238}U or ^{235}U) using Eq. (4). ^{226}Ra can then be calculated using Matlab after obtaining $C_{m,^{230}\text{Th}}$. The program and manual for modeling are provided as **Electronic annexes** to this article.

3. GENERAL BEHAVIOR OF THE MODEL

While we assume that r_a , r_r , and r_c are constants, a more realistic magma differentiation process might treat these as variable; for instance, a fresh magma chamber will likely crystallize faster at its initiation. On the other hand, the assumption that the rate of change of magma mass is a linear function of magma mass implies that a magma chamber could last forever (Touboul et al., 2007). While the most realistic scenario may be between these two end-member models, the general behavior of U-series disequilibria will closely follow the effect of fractional crystallization, ageing, assimilation, and recharge proposed in our model.

3.1. Fractional crystallization and ageing in a closed system (FC)

Because U-series nuclides are generally highly incompatible in most silicate minerals during magma differentiation (e.g., Blundy and Wood, 2003), fractional crystallization itself in a closed system is unlikely to significantly change U-series disequilibria (McKenzie, 1985). However, if the residence time of magma is comparable to the half-life of the short-life nuclides (e.g., ^{226}Ra), radioactive decay will be significant to the disequilibria involving this nuclide. The much shorter half-life of ^{226}Ra means that ($^{226}\text{Ra}/^{230}\text{Th}$) is more sensitive to magma residence time than either the $^{238}\text{U}/^{230}\text{Th}$ or $^{235}\text{U}/^{231}\text{Pa}$ systems. For instance, ^{226}Ra excess dramatically decreases within 2 kyrs due to the ageing effect while ($^{231}\text{Pa}/^{235}\text{U}$) and ($^{238}\text{U}/^{230}\text{Th}$) decrease less than 1% during the same time period (Fig. 2A and B). For a magma chamber with longer residence time (e.g., 20,000 years), where decay removes all initial ^{226}Ra excess, ($^{226}\text{Ra}/^{230}\text{Th}$) of the differentiated melt ($F < 0.4$) is mainly a function of the bulk partition coefficients of Ra and Th. If the fractionated mineral phases include Na-rich plagioclase and amphibole, D_{Ra} will be significantly greater than D_{Th} (Blundy and Wood, 2003) such that fractional crystallization could result in lower $^{226}\text{Ra}/^{230}\text{Th}$ in the melt than in the crystals or whole rock (Reagan et al., 2007).

3.2. Assimilation, fractional crystallization, and ageing (AFC)

In contrast to the closed system, U-Th-Pa-Ra data of the melt in the open system case can be significantly changed by bulk assimilation of crustal materials. Assuming the assimilant is old (in secular equilibrium, e.g., old continental crust), mixing between young magma and older assimilant results in reducing any original U-series disequilibrium signatures (Fig. 3). Within time scales of 200 years to 20k years, ($^{226}\text{Ra}/^{230}\text{Th}$) decreases due to both assimilation and ageing effects (Fig. 3A) while reductions in ($^{238}\text{U}/^{230}\text{Th}$) and

($^{231}\text{Pa}/^{235}\text{U}$) mainly reflect addition of assimilant with lower extents of disequilibria (Fig. 3B). Over a long timescale (e.g., 20,000 years), fractional crystallization could also result in slight ^{226}Ra deficit or excess depending on the difference of the bulk partition coefficients between Ra and Th (Fig. 3A). Because the disequilibria in this model dominantly reflect mixing lines between the original magma and assimilant material with U-series nuclides in secular equilibrium, nearly linear positive correlations between ($^{238}\text{U}/^{230}\text{Th}$) and ($^{226}\text{Ra}/^{230}\text{Th}$) or ($^{231}\text{Pa}/^{235}\text{U}$) are produced (Fig. 3C and D).

3.3. Assimilation, fractional crystallization, ageing, and recharge (AFRCR)

Recharge of new magma into a magma chamber is likely to occur and presents yet another variable in understanding differentiation of magmas. This replenishment is recognized as a trigger for eruption (Sparks et al., 1977) and can dramatically affect the $^{238}\text{U}/^{230}\text{Th}$ – ^{226}Ra disequilibria of erupted lavas by maintaining disequilibria beyond the previously stated five half-life limit of decay (Hughes and Hawkesworth, 1999). Here, we briefly discuss the case of continuous recharge, assuming the added magma has the same chemical composition as the initial magma. Given the same crystallization and/or assimilation rates, a recharging magma chamber model (AFRCR) has lower ($^{238}\text{U}/^{230}\text{Th}$) and higher ($^{226}\text{Ra}/^{230}\text{Th}$) compared with assimilation and fractionation only models (AFC) (Fig. 4). Because the ($^{226}\text{Ra}/^{230}\text{Th}$) of the recharging magma is likely to be high, convergent margin lavas could maintain significant ^{226}Ra excess even when the average magma residence times are greater than 8,000 years. It is important to note that positive correlations between ($^{226}\text{Ra}/^{230}\text{Th}$) and ($^{238}\text{U}/^{230}\text{Th}$) observed in the general AFRCR model ($dM_m/dt \neq 0$) can also be produced in the special ($dM_m/dt = 0$) model given the similar decay effect and assimilation of old crustal material.

4. APPLICATION TO U-SERIES DISEQUILIBRIA IN YOUNG LAVAS FROM CONVERGENT MARGIN

Most lavas at convergent margins are significantly differentiated, justifying our application of the time-dependent AFC model to observed U-series data. However, because important parameters such as r_r , r_a , r_c , and the composition of assimilant are for the most part unconstrained, it is difficult to simulate complicated magma differentiation processes involving crystallization, assimilation, and magma recharge. Regardless, our model can still provide important insights into the correlations between U-series disequilibria and other geochemical features produced by the magma differentiation process. Therefore, we apply our model to intra-oceanic arcs, where the tectonic setting is relatively simple compared to continental subduction zones with significant crustal assimilation. For this case, we only consider fractional crystallization +/- magma recharge to examine the correlations of ^{226}Ra excess with Sr/Th and Ba/Th developed during the time-dependent magma differentiation process. It should be noted that although we focus on intra-oceanic arcs in this paper, the model and equations described above could equally be applied to other tectonic

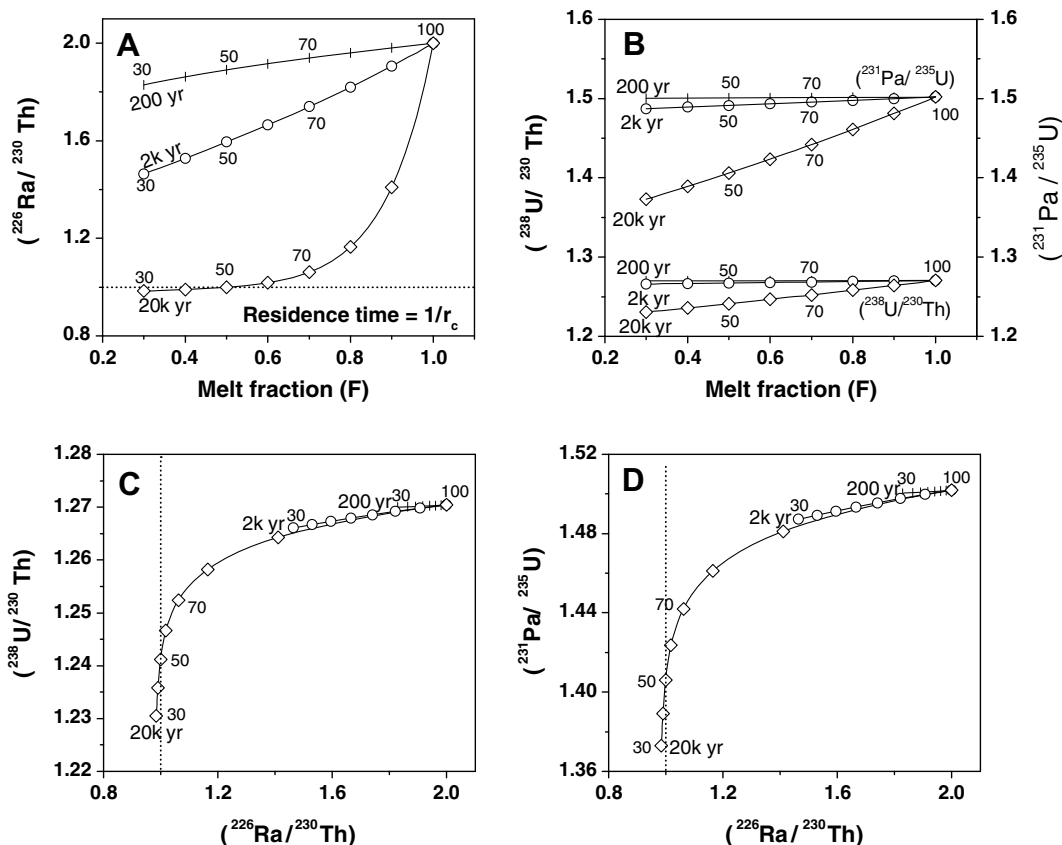


Fig. 2. Results of time-dependent fractional crystallization model (closed system). For simplicity, bulk D of U, Th, and Pa is zero, while bulk D_{Ra} is 0.05. Tick marks denote fraction of the melt (in percentage) in the magma chamber. Residence time = $1/r_c$ (r_c is the crystallization rate). Initial magma: $(^{238}\text{U}/^{230}\text{Th}) = 1.27$, $(^{231}\text{Pa}/^{235}\text{U}) = 1.5$, and $(^{226}\text{Ra}/^{230}\text{Th}) = 2$.

settings such as continental subduction zones, mid-ocean ridges or ocean island settings.

4.1. Choice of partition coefficients

As has been emphasized in previous models (Vigier et al., 1999; Blake and Rogers, 2005), the choice of partition coefficients plays a key role in model results. In this model, we follow the changes in concentration of a few specific trace elements sensitive to fluid additions (e.g., Sr and Ba) as well as U-series nuclides. The choice of crystal-melt partition coefficients for plagioclase and amphibole, the most important mineral phases controlling the behavior of Sr and Ba during convergent margin magma evolution, is the most critical. Partition coefficients for Sr and Ba between plagioclase and silicate melts are a function of both crystal chemical control and melt structure (Blundy and Wood, 1991, 2003; Morse, 1992). Sr is usually compatible in plagioclase while $D_{\text{Ba}}^{\text{plagioclase/melt}}$ varies from greater than one to less than one, depending on plagioclase anorthite content (Blundy and Wood, 1991). Thorium is much more incompatible in plagioclase than either Sr or Ba (Blundy and Wood, 2003). Sr and Ba are moderately incompatible in amphibole while U and Th are highly incompatible (Adam and Green, 1994; Brenan et al., 1995; Latourrette et al., 1995; Blundy and Wood, 2003). Therefore, fractional crystallization of plagioclase and

amphibole can decrease Sr/Th and Ba/Th, but does not change U/Th significantly.

Bulk partition coefficients of trace elements between crystallizing minerals and residual magma are calculated by assuming that the crystallizing assemblage consists of 50% plagioclase, 25% amphibole, plus 25% other minerals in which Sr, Ba, and U-series nuclides are highly incompatible (i.e., partition coefficients ~ 0). This assumption does not affect results significantly. Plagioclase compositions in orogenic andesites vary widely and hence partition coefficients could vary widely. We assume an average plagioclase composition of An_{65} and temperature of 1050 °C based on the most common plagioclase composition in orogenic andesite (Gill, 1981). We calculate $D_{\text{Sr, Ba}}^{\text{plagioclase/melt}}$ using equation 32 and 33 in Blundy and Wood (2003) and $D_{\text{Ra}}^{\text{plagioclase/melt}}$ using the methods provided in Blundy and Wood (2003). Bulk partition coefficients (D_{bulk}) of U, Th, Pa, Ra, Sr, and Ba are listed in Table 2. D_{bulk} for protactinium is assumed to be zero because it should be extremely incompatible in plagioclase and amphibole (Blundy and Wood, 2003).

4.2. The Tonga arc

We chose the well-studied Tonga arc as a case study for modeling AFC process in intra-oceanic arcs. Tonga provides a good example because of an extensive U-series data set and because it exemplifies the positive correlations

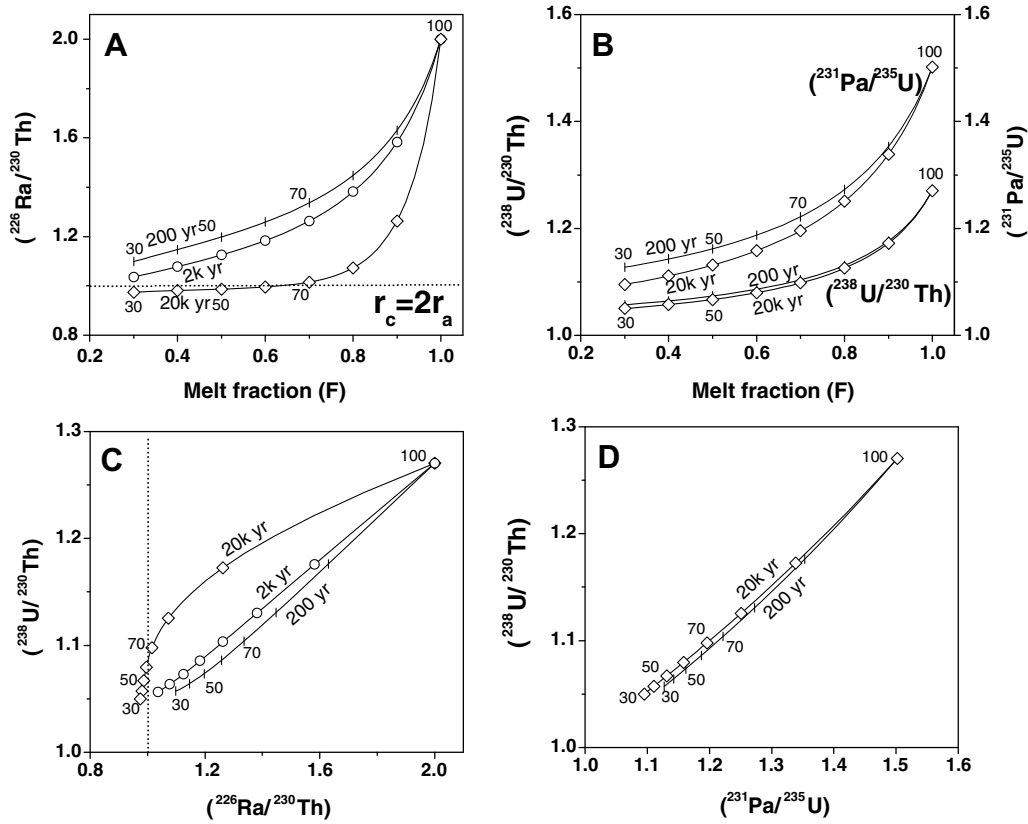


Fig. 3. Results of time-dependent assimilation and fractional crystallization model (open system). Bulk D of U, Th, Pa, and Ra are the same as in Fig. 2. Tick marks denote fraction of the melt (in percentage) in the magma chamber. Assuming $r_c = 2r_a$ (assimilation rate), residence time = $1/(r_c - r_a) = 1/r_a$. Composition of the initial magma: $(^{238}\text{U}/^{230}\text{Th}) = 1.27$, $(^{231}\text{Pa}/^{235}\text{U}) = 1.5$, $(^{226}\text{Ra}/^{230}\text{Th}) = 2$, U = 0.285 ppm, and Th = 0.8 ppm; Crustal assimilate: $(^{238}\text{U}/^{230}\text{Th}) = (^{231}\text{Pa}/^{235}\text{U}) = (^{226}\text{Ra}/^{230}\text{Th}) = 1$, U = 1.2 ppm, and Th = 5 ppm.

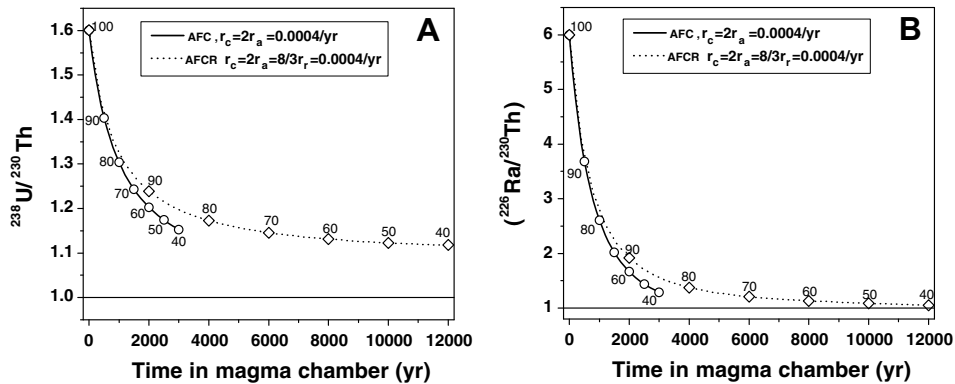


Fig. 4. Comparison of the results from the AFC with the AFRCR model. Recharge of fresh mantle-derived magma can sustain significant ^{226}Ra excess even when the residence time of magma chamber is longer than 8000 years. Initial magma has $(^{238}\text{U}/^{230}\text{Th})$ and $(^{226}\text{Ra}/^{230}\text{Th})$ of 1.6 and 6, respectively. U and Th contents of the initial magma and assimilate are the same as in Fig. 3.

between $(^{226}\text{Ra}/^{230}\text{Th})$ and Sr/Th (or Ba/Th) (Turner et al., 1997, 2000, 2001), used to support the fluid addition model for generation of ^{226}Ra excess in convergent margin lavas. Note that the wide range of both Sr/Th and Ba/Th within only basalt or basaltic andesite samples (<55 wt% SiO_2) from Tonga mainly reflect variations in the mantle source (reflecting the mantle wedge plus fluid or sediment addition) (Fig. 5). Of note here is that more differentiated samples

with known ages and $(^{226}\text{Ra}/^{230}\text{Th})$ data (from Turner et al. (1997, 2000)) show a negative correlation between Sr/Th or Ba/Th (to a lesser extent) and SiO_2 content (except sample 11108 with extremely high Ba/Th). These trends are unlikely to reflect contamination because crustal contamination at shallow depths in intra-oceanic arcs such as the Tonga and Aleutians appears to be insignificant (Turner and Hawkesworth, 1997; Turner et al., 1997, 2000; George

Table 2

Bulk partition coefficients (D) used in the AFCR model

Element	Value	Reference
U	0.001	amp/melt $D_{U,Th,Ba,Sr}$, Latourrette et al. (1995);
Th	0.003	plg/melt D , Blundy and Wood (2003); D_{Ra} is
Pa	0.00	calculated from Blundy and Wood (2003);
Ra	0.03	$D_{Pa} = 0$; Bulk $D = 0.5 \times \text{plg/melt } D + 0.25 \times$
Sr	1.26	amp/melt D
Ba	0.172	

et al., 2003). Therefore, the negative correlation between Sr/Th or Ba/Th and SiO_2 content is most easily explained as fractional crystallization of plagioclase and amphibole (Fig. 5A and B). U/Th shows no correlation with SiO_2 content, consistent with these highly incompatible elements not being affected by plagioclase and amphibole removal (Blundy and Wood, 2003). Therefore, fractional crystallization can substantially decrease Sr/Th and Ba/Th in differentiated arc lavas, while variation of U/Th more likely reflects variations in the mantle source.

Coupling variations in U-series data with Sr/Th and Ba/Th, our model predicts the positive correlations between ($^{226}\text{Ra}/^{230}\text{Th}$) and Sr/Th or Ba/Th. ($^{226}\text{Ra}/^{230}\text{Th}$) in Tongan lavas with known age is positively correlated with Sr/Th and Ba/Th (to a lesser extent neglecting sample 11108) but is uncorrelated with ($^{238}\text{U}/^{230}\text{Th}$) or U/Th (not shown) (Fig. 6) (Turner et al., 1997, 2000). A model of fractional crystallization of plagioclase and amphibole can generally match this trend assuming a crystallization rate from 0.5 to 0.25 kyr^{-1} (i.e., a residence time from 2 to 4 kyrs), which is of the same order of magnitude as the values used in the literature (Vigier et al., 1999; Blake and Rogers, 2005; Touboul et al., 2007). In this model, given the different SiO_2 contents, lavas from individual Tongan islands may have experienced different extents of differentiation. Sr/Th decreases because of crystallization while decay of ^{226}Ra is the dominant cause of ($^{226}\text{Ra}/^{230}\text{Th}$) decreasing and thus the positive correlation (Fig. 6A). The smaller bulk partition coefficient of Ba compared to Sr leads to Ba/Th decreasing at a slower rate than Sr/Th (Fig. 6B). Within a few thousand years, fractional crystallization of plagioclase and amphibole does not significantly change ($^{238}\text{U}/^{230}\text{Th}$) or U/Th (Fig. 6C). Recharge of fresh magma will increase the residence time and ^{226}Ra excess of the magma relative to the fractional crystallization only case with a similar crystallization rate (curve b vs. curve d in Fig. 6A), which also results in the positive correlation between ($^{226}\text{Ra}/^{230}\text{Th}$) and Sr/Th. Therefore, the positive correlations of ($^{226}\text{Ra}/^{230}\text{Th}$) with Sr/Th and Ba/Th could be produced during the time-dependent magma differentiation process.

5. IMPLICATIONS FOR INTERPRETATION OF U-SERIES DISEQUILIBRIA IN SUBDUCTION ZONE LAVAS

Hydrous fluids are generally assumed to transport fluid-mobile elements from the subducted slab to the mantle wedge, resulting in enrichment of large ion lithophile ele-

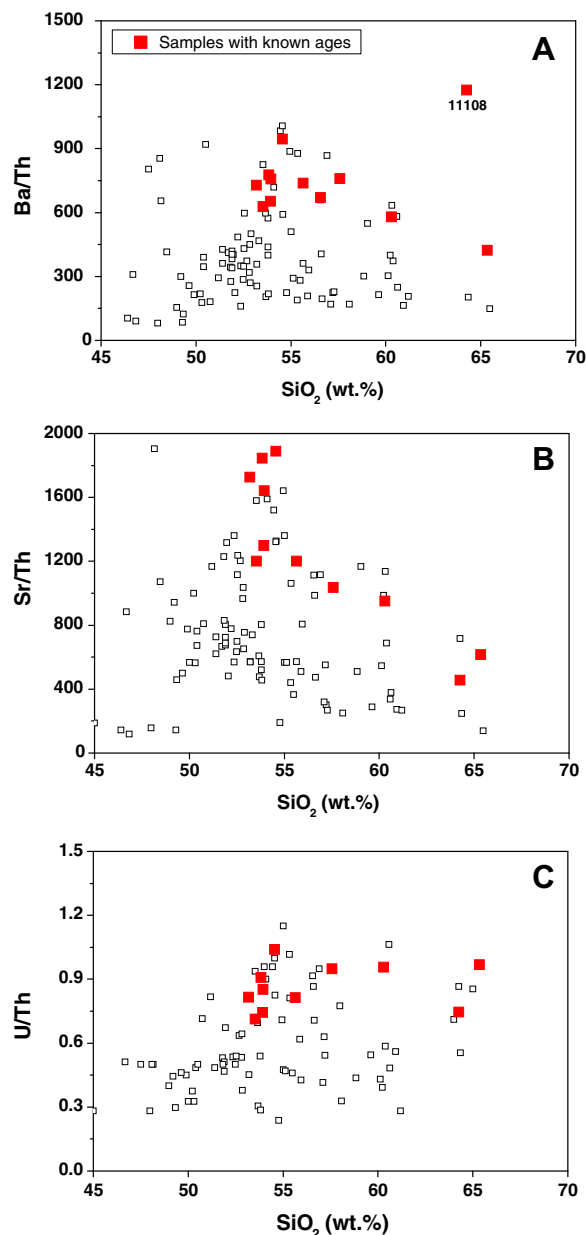


Fig. 5. A, B, and C: Correlations of SiO_2 with commonly used fluid indices (e.g., Sr/Th, Ba/Th, and U/Th) for lavas from the Tonga arc. Solid block symbol data indicated samples with known age (Turner et al., 1997, 2000). Sr/Th and Ba/Th for these samples decrease with increasing SiO_2 content. However, U/Th shows no obvious correlation with SiO_2 . Data are collected from GeoRoc database (<http://georoc.mpch-mainz.gwdg.de/georoc/>). Other data source (open squares) includes Gill (1976, 1984), Ewart et al. (1977, 1994), Vallier et al. (1985), Gill and Whelan (1989), Cole et al. (1990), Wendt et al. (1997), Luttinen and Furnes (2000) and Turner et al. (1997, 2000).

ments (e.g., U and Ba) relative to other less mobile elements in lavas from subduction zones. Increased ratios of fluid-mobile elements (e.g., Sr, Ba, U, and Ra) over fluid-immobile elements (e.g., Th) can be considered as indicators of fluid addition. Addition of varying amounts of fluid to

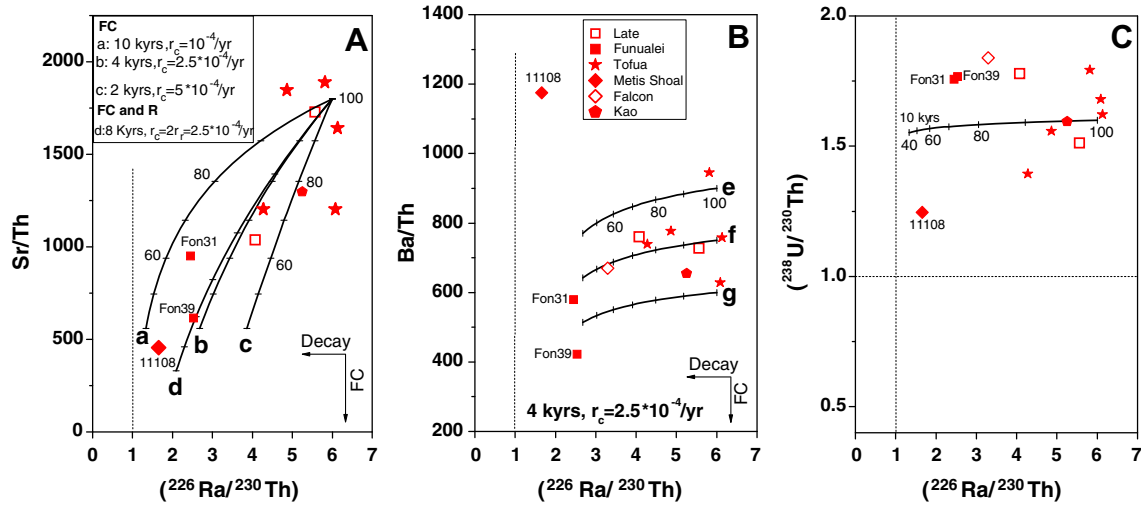


Fig. 6. Simulating the relationships of $(^{226}\text{Ra}/^{230}\text{Th})$ with Sr/Th, Ba/Th, and U/Th produced during fractional crystallization (FC) and recharge (R). (A) $(^{226}\text{Ra}/^{230}\text{Th})$ vs. Sr/Th. Curves a, b, and c represent pure fractional crystallization model with residence time of 10, 4, and 2 kyrs, respectively. Curve d in (A) describes fractional crystallization and recharge of fresh magma assuming that $r_c = 2r_r = 2.5 \times 10^{-4}/\text{yr}$; (B) $(^{226}\text{Ra}/^{230}\text{Th})$ vs. Ba/Th. Curves e, f, and g in (B) use Ba/Th of 900, 750, and 600, respectively; (C) $(^{226}\text{Ra}/^{230}\text{Th})$ vs. U/Th. $(^{226}\text{Ra}/^{230}\text{Th})$ of the Tonga samples is positively correlated with Sr/Th and Ba/Th (to a lesser extent), but shows no obvious correlation with $(^{238}\text{U}/^{230}\text{Th})$. However, the model does show that $(^{238}\text{U}/^{230}\text{Th})$ decreases slightly by $\sim 3\%$ due to decay when the residence time is 10 thousand years. Only Tonga samples with known eruption ages are plotted and grouped based on the sample locations (Turner et al., 1997, 2000). The positive correlations between $(^{226}\text{Ra}/^{230}\text{Th})$ and Sr/Th or Ba/Th can be explained by different extents of differentiation. Fraction of magma remaining (F) is marked in percentage (%). Parameters of simulation are from Table 3.

the mantle wedge beneath arc front volcanoes could thus cause the positive correlations observed between Ba/Th, Sr/Th, and $(^{226}\text{Ra}/^{230}\text{Th})$. Therefore, for more than a decade, these correlations have been considered as the strongest evidence supporting the generation of ^{226}Ra excess in subduction zone lavas by Ra-rich fluid addition (e.g., Turner and Hawkesworth, 1997; Turner et al., 2000, 2003; Turner and Foden, 2001; Sigmarsson et al., 2002; George et al., 2003, 2004). Moreover, to preserve the fluid-based ^{226}Ra excess, which is only produced at the slab-wedge interface, ultra-fast magma ascent rates (up to the order of 1000 meter per year) are required (Hawkesworth et al., 1997; Turner et al., 2001, 2003; Turner and Foden, 2001; George et al., 2003, 2004).

The good match between the Tongan data and our time-dependent AFC model shows that correlations between $(^{226}\text{Ra}/^{230}\text{Th})$ and Ba/Th, and Sr/Th do not provide unambiguous evidence for ^{226}Ra excess in subduction zone lavas

reflecting fluid addition. Instead, these correlations can be equally explained by crustal level differentiation processes thus relaxing constraints on timescales of magmatism and melt ascent rate. The anti-correlation between $(^{226}\text{Ra}/^{230}\text{Th})$ and SiO_2 (e.g., Fig. 2 in Turner et al., 2001) indicates that more primitive subduction zone magmas have larger ^{226}Ra excesses, higher Ba/Th and Sr/Th, and relatively lower SiO_2 contents. Magma differentiation with time at shallow crustal depths decreases ^{226}Ra excess, Ba/Th, and Sr/Th, and increases SiO_2 , producing the correlations of ^{226}Ra excess with Ba/Th, Sr/Th, and SiO_2 content in young lavas from subduction zones (Fig. 6).

Clearly, the observation that ^{226}Ra excesses are highest in more primitive magmas argues that they present when they arrive at crustal level magma chambers. While it is still possible they could reflect fluid addition, there are many other processes that could equally well produce the ^{226}Ra excesses prior to differentiation. For instance, in-growth melting models have been proposed to explain other U-series disequilibria (Turner et al., 2006; Huang and Lundstrom, 2007); if such processes occur to produce ^{231}Pa – ^{235}U disequilibria, it is likely that they also act to produce ^{226}Ra – ^{230}Th disequilibria if D_{Ra} is not equal to D_{Th} and one of them has a bulk partition coefficient of similar size to the melt porosity. Diffusive exchange between minerals in the mantle wedge (Feineman and DePaolo, 2003) or incongruent melting in the lower crust (Dufek and Cooper, 2005) are also viable processes for producing ^{226}Ra excess before arrival at crustal magma chambers. Therefore, if any of these other mechanisms act to produce ^{226}Ra excess prior to differentiation, then the constraint on the ultra-fast magma upwelling from the upper mantle to Earth's surface is eliminated. If

Table 3
Trace element and U-series data used in Fig. 6

	Primary magma
C_{U} (ppm)	0.4
C_{Th} (ppm)	1
C_{Sr} (ppm)	1800
C_{Ba} (ppm)	600, 750, 900
$(^{238}\text{U}/^{230}\text{Th})$	1.6
$(^{230}\text{Th}/^{232}\text{Th})$	0.76
$(^{231}\text{Pa}/^{235}\text{U})$	1.2
$(^{226}\text{Ra}/^{230}\text{Th})$	6

correlations between ^{226}Ra excess and Sr/Th or Ba/Th simply reflect differentiation processes, the cause of ^{226}Ra excess in subduction zone lavas and thus magma transfer time-scale are still open questions.

6. CONCLUSIONS

Models of time-dependant AFC process indicate that U-series disequilibria in young lavas at the convergent margins can be significantly affected by the magma differentiation process of fractional crystallization, assimilation, magma recharge, and ageing. In a closed system, U-series disequilibria are dominantly changed by the ageing effect because U-series nuclides are generally highly incompatible during differentiation. Within a few thousand years, this process does not change U/Th and ($^{238}\text{U}/^{230}\text{Th}$). In an open system, assimilation of old crustal material can lessen the primary U-series disequilibria, while recharge of fresh magma produced from the deep mantle can maintain U-series disequilibria in magmas crustal residence times greater than five half-lives.

The positive correlations between ^{226}Ra excess and Sr/Th or Ba/Th (to a lesser extent) have been widely used as evidence supporting the generation of ^{226}Ra excess in convergent margin lavas by fluid additions. Our model shows that these positive correlations can equally be explained by fractional crystallization of plagioclase and amphibole coupled with contemporaneous decay of ^{226}Ra . Therefore, the correlations between chemical parameters sensitive to fluid addition (e.g., Sr/Th and Ba/Th) and ($^{226}\text{Ra}/^{230}\text{Th}$) cannot be exclusively used to support the fluid addition model. Recent fluid addition and ultra-fast ascent rates of magmas may not be required for generation and preservation of ^{226}Ra excess in young subduction zone lavas.

ACKNOWLEDGMENTS

We are grateful to Chunguang Xia for improving the Matlab program and Mark Reagan for helpful discussions. O. Sigmarrsson, J. Dufek, and an anonymous reviewer are thanked for their insightful comments, which greatly improved the manuscript. We thank P. Ulmer for editorial handling and instructive comments.

APPENDIX A. SUPPLEMENTARY DATA

Supplementary data associated with this article can be found, in the online version, at doi:10.1016/j.gca.2008.05.060.

REFERENCES

- Adam J. and Green T. H. (1994) The effects of pressure and temperature on the partitioning of Ti, Sr and REE between amphibole, clinopyroxene and basanitic melts. *Chem. Geol.* **117**, 219–233.
- Asmerom Y., Dufrane S. A., Mukasa S. B., Cheng H. and Edwards R. L. (2005) Timescale of magma differentiation in arcs from protactinium-radium isotopic data. *Geology* **33**, 633–636.
- Beard J. S., Ragland P. C. and Crawford M. L. (2005) Reactive bulk assimilation: A model for crust-mantle mixing in silicic magmas. *Geology* **33**, 681–684.
- Blake S. and Rogers N. (2005) Magma differentiation rates from ($^{226}\text{Ra}/^{230}\text{Th}$) and the size and power output of magma chambers. *Earth Planet. Sci. Lett.* **236**, 654–669.
- Blundy J. and Wood B. (2003) Mineral–melt partitioning of Uranium, Thorium and their daughters. *Rev. Mineral. Geochem.* **52**, 59–123.
- Blundy J. D. and Wood B. J. (1991) Crystal–chemical controls on the partitioning of Sr and Ba between plagioclase feldspar, silicate melts, and hydrothermal solutions. *Geochim. Cosmochim. Acta* **55**, 193–209.
- Bourdon B., Turner S. and Allègre C. (1999) Melting dynamics beneath the Tonga-Kermadec island arc inferred from ^{231}Pa – ^{235}U systematics. *Science* **286**, 2491–2493.
- Brenan J. M., Shaw H. F., Ryerson F. J. and Phinney D. L. (1995) Experimental determination of trace-element partitioning between pargasite and a synthetic hydrous andesitic melt. *Earth Planet. Sci. Lett.* **135**, 1–11.
- Cole J. W., Graham I. J. and Gibson I. L. (1990) Magmatic evolution of later Cenozoic volcanic rocks of the Lau ridge, Fiji. *Contrib. Mineral. Petrol.* **104**, 540–554.
- Condomines M., Tanguy J.-C. and Michaud V. (1995) Magma dynamics at Mt. Etna: constraints from U–Th–Ra–Pb radioactive disequilibria and Sr isotopes in historical lavas. *Earth Planet. Sci. Lett.* **132**, 25–41.
- Condomines M., Gauthier P.-J. and Sigmarrsson O. (2003) Timescales of magma chamber processes and dating of young volcanic rocks. *Review in Mineralogy and Geochemistry* **52**, 126–174.
- Cooper K. M., Reid M. R., Murrell M. T. and Clague D. A. (2001) Crystal and magma residence at Kilauea Volcano, Hawaii: ^{230}Th – ^{226}Ra dating of the 1955 east rift eruption. *Earth Planet. Sci. Lett.* **184**, 703–718.
- DePaolo D. J. (1981) Trace element and isotopic effects of combined wallrock assimilation and fractional crystallization. *Earth Planet. Sci. Lett.* **53**, 189–202.
- Dosseto A., Bourdon B., Joron J.-L. and Dupré B. (2003) U–Th–Pa–Ra study of the Kamchatka arc: new constraints on the genesis of arc lavas. *Geochim. Cosmochim. Acta* **67**, 2857–2877.
- Dufek J. and Cooper K. M. (2005) $^{226}\text{Ra}/^{230}\text{Th}$ excess generated in the lower crust: implications for magma transport and storage timescales. *Geology* **37**, 833–836.
- Ewart A., Brothers R. N. and Mategan A. (1977) An outline of the geology and geochemistry, and the possible petrogenetic evolution of the volcanic rocks of the Tonga–Kermadec–New Zealand island arc. *J. Volcanol. Geotherm. Res.* **2**, 205–250.
- Ewart A., Bryan W. B., Chappell B. W. and Rudnick R. L. (1994) Regional geochemistry of the Lau-Tonga arc and back-arc systems. *Proc. Ocean Drill. Program., Sci. Results* **135**, 385–425.
- Feineman M. D. and DePaolo D. J. (2003) Steady-state $^{226}\text{Ra}/^{230}\text{Th}$ disequilibrium in mantle minerals: implications for melt transport rates in island arcs. *Earth Planet. Sci. Lett.* **215**, 339–355.
- George R., Reagan M., Turner S., Gill J. and Bourdon B. (2004) Comment on “Steady-state $^{226}\text{Ra}/^{230}\text{Th}$ disequilibrium in mantle minerals: implications for melt transport rates in island arcs” by M.D. Feineman and D.J. DePaolo [Earth Planet. Sci. Lett. 215 (2003) 339–355]. *Earth Planet. Sci. Lett.* **228**, 563–567.
- George R., Turner S., Hawkesworth C., Morris J., Nye C., Ryan J. and Zheng S.-H. (2003) Melting processes and fluid and sediment transport rates along the Alaska–Aleutian arc from an integrated U–Th–Ra–Be isotope study. *J. Geophys. Res.* **108**(B5), 2252.
- Gill J. B. (1976) Composition and age of Lau Basin and ridge volcanic rocks: implications for evolution of an interarc basin and remnant arc. *Bull. Geol. Soc. Am.* **87**, 1384–1395.

- Gill J. B. (1981) *Orogenic Andesites and Plate Tectonics*. Springer-Verlag, Berlin.
- Gill J. B. (1984) Sr–Pb–Nd isotopic evidence that both MORB and OIB sources contribute to oceanic island arc magmas in Fiji. *Earth Planet. Sci. Lett.* **68**, 443–458.
- Gill J. B. and Whelan P. M. (1989) Early rifting of an oceanic island arc (Fiji) produced shoshonitic to tholeiitic basalts. *J. Geophys. Res.* **B94**, 4561–4578.
- Grove T. L., Chatterjee N., Parman S. W. and Médard E. (2006) The influence of H₂O on mantle wedge melting. *Earth Planet. Sci. Lett.* **249**, 74–89.
- Grove T. L. and Kinzler R. J. (1986) Petrogenesis of andesites. *Ann. Rev. Earth Planet. Sci.* **14**, 417–454.
- Halliday A. N., Mahood G. A., Holden P., Metz J. M., Dempster T. J. and Davidson J. P. (1989) Evidence for long residence times of rhyolitic magma in the Long Valley magmatic system: the isotopic record in precaldera lavas of Glass Mountain. *Earth Planet. Sci. Lett.* **94**, 274–290.
- Hawkesworth C. J., Blake S., Evans P., Hughes R., Macdonald R., Thomas L. E., Turner S. P. and Zellmer G. (2000) Timescales of crystal fractionation in magma chambers—integrating physical, isotopic and geochemical perspectives. *J. Petrol.* **41**, 991–1006.
- Hawkesworth C. J., Turner S. P., Mcdermott F., Peate D. W. and Calsteren P. V. (1997) U–Th isotopes in Arc magmas: implications for element transfer from the subducted crust. *Science* **412**, 501–507.
- Heath E., Turner S. P., Macdonald R., Hawkesworth C. J. and Calsteren P. V. (1998) Long magma residence times at an island arc volcano (Soufriere, St. Vincent) in the Lesser Antilles: evidence from ²³⁸U–²³⁰Th isochron dating. *Earth Planet. Sci. Lett.* **160**, 49–63.
- Hildreth W. and Moorbath S. (1988) Crustal contributions to arc magmatism in the Andes of Central Chile. *Contrib. Mineral. Petrol.* **98**, 455–489.
- Huang F. and Lundstrom C. C. (2007) ²³¹Pa excesses in arc volcanic rocks: constraint on melting rates at convergent margins. *Geology* **35**, 1007–1010.
- Hughes R. D. and Hawkesworth C. J. (1999) The effects of magma replenishment processes on ²³⁸U–²³⁰Th disequilibrium. *Geochim. Cosmochim. Acta* **63**, 4101–4110.
- Jicha B. R., Singer B. S., Beard B. L. and Johnson C. M. (2005) Contrasting timescales of crystallization and magma storage beneath the Aleutian Island arc. *Earth Planet. Sci. Lett.* **236**, 195–210.
- Latourrette T., Hervig R. L. and Holloway J. R. (1995) Trace element partitioning between amphibole, phlogopite, and basanite melt. *Earth Planet. Sci. Lett.* **135**, 13–30.
- Luttinen A. V. and Furnes H. (2000) Flood basalts of Vestfjella Jurassic magmatism across an Archaean–Proterozoic lithospheric boundary in Dronning Maud Land, Antarctica. *J. Petrol.* **41**, 1271–1305.
- McKenzie D. (1985) ²³⁰Th–²³⁸U disequilibrium and the melting process beneath ridge axes. *Earth Planet. Sci. Lett.* **72**, 149–157.
- Morse S. A. (1992) Partitioning of strontium between plagioclase and melt: a comment. *Geochim. Cosmochim. Acta* **56**, 1735–1737.
- Pickett D. A. and Murrell M. T. (1997) Observation of ²³¹Pa/²³⁵U disequilibrium in volcanic rocks. *Earth Planet. Sci. Lett.* **148**, 259–271.
- Reagan M. K., Sims K. W. W., Erich J., Thomas R. B., Cheng H., Edwards R. L., Layne G. and Ball L. (2003) Time-scales of differentiation from mafic parents to rhyolite in North American continental arcs. *J. Petrol.* **44**, 1703–1726.
- Reagan M. K., Turner S., Legg M., Sims K. W. W. and Hards V. L. (2007) ²³⁸U- and ²³²Th-decay series constraints on the timescales of generation and degassing for phonolite erupted in 2004 near Tristan da Cunha. *Goldschmidt Conference Abstracts*.
- Sigmarrsson O., Chmeleff J., Morris J. and Lopez-Escobar L. (2002) Origin of ²²⁶Ra–²³⁰Th disequilibria in arc lavas from southern Chile and implications for magma transfer time. *Earth Planet. Sci. Lett.* **196**, 189–196.
- Sparks R. S. J., Sigurdsson H. and Wilson L. (1977) Magma mixing: a mechanism for triggering acid explosive eruptions. *Nature* **267**, 315–318.
- Thomas R. B., Hirschmann M. M., Cheng H., Reagan M. K. and Edwards R. L. (2002) (²³¹Pa/²³⁵U)–(²³⁰Th/²³⁸U) of young mafic volcanic rocks from Nicaragua and Costa Rica and the influence of flux melting on U-series systematics of arc lavas. *Geochim. Cosmochim. Acta* **66**, 4287–4309.
- Touboul M., Bourdon B., Villemant B., Boudon G. and Jean-Louis J. (2007) ²³⁸U–²³⁰Th–²²⁶Ra disequilibria in andesitic lavas of the last magmatic eruption of Guadeloupe Soufriere, French Antilles: processes and timescales of Magma differentiation. *Chem. Geol.* **246**, 181–206.
- Turner S., Bourdon B. and Gill J. (2003) U-series isotopes and magma genesis at convergent margins. *Rev. Mineral. Geochem.* **52**, 255–315.
- Turner S., Bourdon B., Hawkesworth C. and Evans P. (2000) ²²⁶Ra–²³⁰Th evidence for multiple dehydration events, rapid melt ascent and the timescales of differentiation beneath the Tonga–Kermadec island arc. *Earth Planet. Sci. Lett.* **179**, 581–593.
- Turner S., Evans P. and Hawkesworth C. (2001) Ultrafast source-to-surface movement of melt at island arcs from ²²⁶Ra–²³⁰Th systematics. *Science* **292**, 1363–1366.
- Turner S. and Foden J. (2001) U, Th and Ra disequilibria, Sr, Nd and Pb isotope and trace element variations in Sunda arc lavas: predominance of a subducted sediment component. *Contrib. Mineral. Petrol.* **142**, 43–57.
- Turner S. and Hawkesworth C. (1997) Constraints on flux rates and mantle dynamics beneath island arcs from Tonga–Kermadec lava geochemistry. *Nature* **389**, 568–573.
- Turner S., Hawkesworth C., Calsteren P. V., Heath E., Macdonald R. and Black S. (1996) U-series isotopes and destructive plate margin magma genesis in the Lesser Antilles. *Earth Planet. Sci. Lett.* **142**, 191–207.
- Turner S., Hawkesworth C., Rogers N., Bartlett J., Worthington T., Hergt J., Pearce J. and Smith I. (1997) ²³⁸U–²³⁰Th disequilibria, magma petrogenesis, and flux rates beneath the depleted Tonga–Kermadec island arc. *Geochim. Cosmochim. Acta* **61**, 4855–4884.
- Turner S., Regelous M., Hawkesworth C. and Rostami K. (2006) Partial melting processes above subducting plates: constraints from ²³¹Pa–²³⁵U disequilibria. *Geochim. Cosmochim. Acta* **70**, 480–503.
- Vallier T. L., Stevenson A. J. and Scholl D. W. (1985) Petrology of igneous rocks from Ata Island, Kindon of Tonga. In *Geology and Offshore Resources of Pacific Island Arcs—Tonga region* eds. (D. W. Scholl and T. L. Vallier). Circum-Pacific Council for Energy of Mineral Resources, Houston, Texas, pp. 301–316.
- Vigier N., Bourdon B., Joron J. L. and Allegre C. J. (1999) U-decay series and trace element systematics in the 1978 eruption of Ardoukoba, Asal rift: timescale of magma crystallization. *Earth Planet. Sci. Lett.* **174**, 81–97.
- Wendt J. I., Regelous M., Collerson K. D. and Ewart A. (1997) Evidence for the role of two mantle plumes in island arc lavas from Northern Tonga. *Geology* **25**, 611–614.
- Zellmer G., Turner S. and Hawkesworth C. (2000) Timescales of destructive plate margin magmatism new insights from Santorini, Aegean volcanic arc. *Earth Planet. Sci. Lett.* **174**, 265–281.